Engineering 6 (2020) 165–172

Contents lists available at ScienceDirect

Engineering

journal homepage: www.elsevier.com/locate/eng

Research
Rare Earth Permanent Magnets—Article

An Efficient Process for Recycling Nd–Fe–B Sludge as High-Performance Sintered Magnets

Xiaowen Yin [a], Ming Yue [a,b,c,*], Qingmei Lu [a,c], Min Liu [a,c], Feng Wang [a], Yubing Qiu [a], Weiqiang Liu [a,b,c], Tieyong Zuo [a,c], Shanshun Zha [b,d], Xuliang Li [b,d], Xiaofei Yi [b,d]

[a] College of Materials Science and Engineering, Beijing University of Technology, Beijing 100124, China
[b] State Key Laboratory of Rare Earth Permanent Magnetic Materials, Hefei 231500, China
[c] Key Laboratory of Advanced Functional Materials, Ministry of Education, Beijing University of Technology, Beijing 100124, China
[d] Earth-Panda Advanced Magnetic Materials Co., Ltd., Hefei 231500, China

ARTICLE INFO

Article history:
Received 13 August 2018
Revised 5 January 2019
Accepted 15 April 2019
Available online 21 November 2019

Keywords:
Nd–Fe–B grinding sludge
Recycled sintered magnets
Calcium reduction–diffusion
Rare-earth-rich alloy doping

ABSTRACT

Given the increasing concern regarding the global decline in rare earth reserves and the environmental burden from current wet-process recycling techniques, it is urgent to develop an efficient recycling technique for leftover sludge from the manufacturing process of neodymium–iron–boron (Nd–Fe–B) sintered magnets. In the present study, centerless grinding sludge from the Nd–Fe–B sintered magnet machining process was selected as the starting material. The sludge was subjected to a reduction–diffusion (RD) process in order to synthesize recycled neodymium magnet ($Nd_2Fe_{14}B$) powder; during this process, most of the valuable elements, including neodymium (Nd), praseodymium (Pr), gadolinium (Gd), dysprosium (Dy), holmium (Ho), and cobalt (Co), were recovered simultaneously. Calcium chloride ($CaCl_2$) powder with a lower melting point was introduced into the RD process to reduce recycling cost and improve recycling efficiency. The mechanism of the reactions was investigated systematically by adjusting the reaction temperature and calcium/sludge weight ratio. It was found that single-phase $Nd_2Fe_{14}B$ particles with good crystallinity were obtained when the calcium weight ratio (calcium/sludge) and reaction temperature were 40 wt% and 1050 °C, respectively. The recovered $Nd_2Fe_{14}B$ particles were blended with 37.7 wt% $Nd_4Fe_{14}B$ powder to fabricate Nd–Fe–B sintered magnets with a remanence of 12.1 kG (1 G = 1×10^{-4} T), and a coercivity of 14.6 kOe (1 Oe = 79.6 $A \cdot m^{-1}$), resulting in an energy product of 34.5 MGOe. This recycling route promises a great advantage in recycling efficiency as well as in cost.

1. Introduction

Green energy is playing an increasingly important role in modern society. Some forms of green energy require strong support from permanent magnet (PM) materials, such as ferrite, alnico, samarium cobalt, and neodymium–iron–boron (Nd–Fe–B) [1,2]. Nd–Fe–B sintered magnets are the most popular choice, as they possess the highest energy product of all commercial PM materials [3,4]. With the development of clean energy equipment such as wind turbines and hybrid electric vehicles, the consumption of Nd–Fe–B sintered magnets is growing yearly, and reached a global level of 132.8 kt in 2016 [5]. To obtain final products of a desirable size, Nd–Fe–B sintered magnets are subjected to various machining processes, including wire-electrode cutting, slicing, and centerless grinding. During these manufacturing processes, about 25 wt% of scraps are generated [6]. More than 30 wt% of rare earth elements (REEs) are contained in the Nd–Fe–B scraps, including neodymium (Nd), praseodymium (Pr), gadolinium (Gd), dysprosium (Dy), terbium (Tb), and holmium (Ho), which are all essential elements in various industrial applications. The recycling of Nd–Fe–B scraps is thus an important part of maintaining a sustainable supply chain for REEs.

Nd–Fe–B scraps usually contain irregular bulk scraps and sludge. Hydrogen decrepitation (HD) has been conducted on irregular bulk scraps to obtain recycled Nd–Fe–B sintered magnets, and has proven to be a potential route for commercial-scale application [7,8]. However, Nd–Fe–B sludge has mainly been used as a valuable secondary resource for the recovery of REEs. The selective extraction of REEs is the major aim in recycling Nd–Fe–B sludge. Comprehensive reviews have summarized the approaches taken thus far to recover REEs from sludge [9,10]. Wet chemical

* Corresponding author.
E-mail address: yueming@bjut.edu.cn (M. Yue).

https://doi.org/10.1016/j.eng.2019.11.007

processes are generally preferred; these processes usually consist of complete dissolution of Nd–Fe–B sludge in an acid, followed by selective precipitation of the REEs as sulfates or fluorides. Such recycling processes consume a large amount of chemicals such as hydrochloric acid (HCl), sulphuric acid (H_2SO_4), hydrofluoric acid (HF), and sodium hydroxide (NaOH), and generate considerable volumes of waste water [11–13], thereby creating a heavy environmental burden [14]. On the other hand, pyrometallurgical processes such as selective chlorination, vacuum induction melting, thermal isolation, and roasting can selectively and efficiently extract REEs from Nd–Fe–B scraps [15,16]. However, these recycling processes are always operated at a high temperature above 950 °C and are thus quite energy intensive and expensive.

In addition to the rare earths, other valuable elements are contained in the Nd–Fe–B sludge, such as cobalt (Co), gallium (Ga), zirconium (Zr), and niobium (Nb). However, Nd–Fe–B sludge is usually severely contaminated by the cutting fluid and other impurities during the machining processes, and thus exhibits high oxygen content. Calcium (Ca) metal has a strong thermodynamic affinity with oxygen, and has been applied to synthesize neodymium magnet ($Nd_2Fe_{14}B$) powder through the reduction–diffusion (RD) process [17]. This process provides a potential route for the recycling of the sludge. An effective method was proposed in Refs. [18–21] to recycle Nd–Fe–B sludge as bonded magnets without acid; this method involves removing carbon by heating the sludge at a high temperature in air, and subsequently reducing oxygen through a calcium RD process. Based on this method, our group obtained recycled Nd–Fe–B sintered magnets from the sludge. The sludge was pretreated by distillation to remove organic impurities and then used to synthesize $Nd_2Fe_{14}B$ powder via the RD process. After doping with rare earth hydride, recycled Nd–Fe–B sintered magnets with good magnetic properties were prepared through sintering. The best magnetic properties of the recycled Nd–Fe–B sintered magnets—namely, a remanence of 12.2 kG (1 G = 1×10^{-4} T), coercivity of 10.3 kOe (1 Oe = 79.6 $A \cdot m^{-1}$), and energy product of 35.2 MGOe—were recovered from the sludge through doping with 10 wt% of hydroneodymium compound (NdH_x) particles. It was also found that the RD process has advantages when recycling Nd–Fe–B sludge in comparison with the conventional recycling process: It is more environmentally friendly, energy saving, and high efficiency, as we have reported in detail [22,23].

Although the Nd–Fe–B sludge can be successfully recovered as magnets by the RD process, the mechanism of the RD process, recycling efficiency, and cost have not been further discussed. In this study, we have designed an efficient recycling route for Nd–Fe–B sludge in order to address these points. Centerless grinding Nd–Fe–B sludge was selected as the starting material from a variety of sludges in order to improve the recycling efficiency. Calcium chloride ($CaCl_2$) powder was introduced to assist the chemical reactions and reduce the usage of calcium granules, thereby reducing the recycling cost. In order to systematically investigate the mechanism of the RD process, the reaction temperature and calcium/sludge ratio were adjusted in this study. Moreover, $Nd_4Fe_{14}B$ powder was doped into the recycled powder as a rare-earth-rich alloy during the sintering process in order to achieve a high magnetic performance, which can also improve the utilization efficiency of rare earths and reduce the recycling cost. Furthermore, the application of a rare-earth-rich alloy in the sintered process increases the feasibility of industrial applications.

2. Materials and methods

The Nd–Fe–B sludge was obtained from Anhui Earth-Panda Advance Magnetic Material Co. Ltd., and was stored in a plastic sealed barrel with ethyl alcohol. Fig. 1 shows the recycling route of the Nd–Fe–B sludge in this study. Before the RD process, the sludge was dried at 60 °C for 2 h in air. The dried sludge, Ca granules, and $CaCl_2$ powder were mixed and loaded in a stainless-steel crucible under an argon (Ar) atmosphere. $CaCl_2$ powder was added as a fluxing agent to ensure full reduction. Reaction mixtures with a calcium/sludge weight ratio of 20 wt%, 30 wt%, 40 wt%, and 50 wt%, respectively, were prepared and mixed with 30 wt% of $CaCl_2$ powder. The calcium/sludge weight ratios were decided by the oxygen content of the sludge, as mentioned below. To study the reaction mechanism of the RD process, reaction temperatures of 600, 850, 950, and 1050 °C, respectively, were conducted for 2 h with the optimal calcium/sludge weight ratio. After the RD process, the samples were washed with ice water under a nitrogen atmosphere for 1 h to remove calcium oxide (CaO), calcium chloride hydroxide (CaClOH), and residual Ca, and then dried in a vacuum.

To obtain recycled Nd–Fe–B sintered magnets, $Nd_2Fe_{14}B$ powder recovered from the sludge was blended with $Nd_4Fe_{14}B$ powder for sintering. Appropriate size distribution of the recycled $Nd_2Fe_{14}B$ powder was achieved through 90 min of ball milling with a ball-to-powder ratio of 10:1. The $Nd_4Fe_{14}B$ powder was prepared through smelting, HD, and a jet-milling process. Because the rare earth content of the recovered $Nd_2Fe_{14}B$ powder decreased after the RD process, the milled powder was mixed with different amounts of $Nd_4Fe_{14}B$ powder, ranging from 33.3 wt% to 45.8 wt%, and then pressed together under a magnetic field of 2 T. The green compacts were sintered at 1090 °C for 3 h under a vacuum of 1×10^{-3} Pa; they were subsequently annealed at 900 °C for 3 h and then at 480 °C for 2 h.

The chemical composition and crystal structure of the Nd–Fe–B sludge, RD-treated $Nd_2Fe_{14}B$ powders, and final recycled magnets were determined with an inductively coupled plasma optical emission spectrometer (ICP-OES), a C–H–O elemental analyzer, and X-ray diffraction (XRD) with Cu-Kα radiation. The morphology of the sludge powder, RD-treated powders, ball-milled powder, and $Nd_4Fe_{14}B$ powder and the microstructure of the recycled Nd–Fe–B sintered magnets were observed using scanning electron

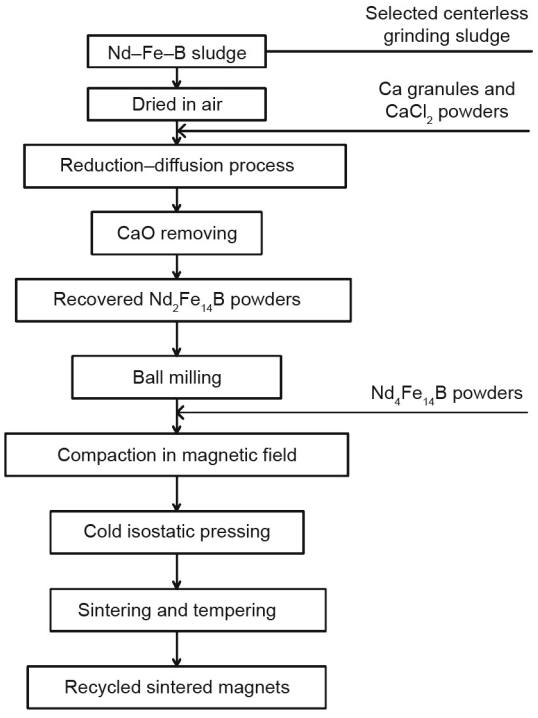

Fig. 1. Schematics of the recycling process of Nd–Fe–B sludge.

microscopy (SEM). The particle sizes of the ball-milled powder and the $Nd_4Fe_{14}B$ powder were examined with a laser particle size analyzer (LPSA). The magnetic properties of the recycled magnets were measured with a *B–H* loop tracer, and the densities of the magnets were determined by the Archimedes method.

3. Results and discussion

3.1. Characterization of Nd–Fe–B centerless grinding sludge

To obtain a product with a desirable size, numerous machining processes are necessary in the preparation of sintered magnets. These processes include grinding, slicing, centerless grinding, trepanning, and wire-electrode cutting. During the machining process, some processes require high temperatures and use organic cooling liquid, such as the wire-electrode cutting process. Therefore, the sludge obtained from the wire-electrode cutting process is severely contaminated and oxidized. The raw material selected in this study was Nd–Fe–B centerless grinding sludge, which is generated from the centerless grinding process with water cooling. To reduce the surface roughness of the cylindrical product, the centerless grinding process is conducted on the surface of the magnets.

Fig. 2 shows the morphology, XRD pattern, and chemical composition of Nd–Fe–B centerless grinding sludge that was dried at 60 °C for 2 h in air. As shown in Fig. 2(a), the particles do not have sharp edges, and needle-like and hexagonal flaky particles appear on the surface of the sludge powder. The sludge powder is composed of hydrogen neodymium oxide ($Nd(OH)_3$) and ferroferric oxide (Fe_3O_4), as determined by the XRD scan shown in Fig. 2(b). The core of the large sludge particles is composed of $Nd_2Fe_{14}B$ hydride ($Nd_2Fe_{14}BH_x$). Since the cooling liquid is water, less impurity remains in the centerless grinding sludge, aside from oxygen and hydrogen, as shown in Fig. 2(c). Due to various grades of Nd–Fe–B sintered magnets being processed in the same machine, the chemical composition of the sludge is complex, and contains the rare earths Nd, Pr, Gd, Dy, and Ho; the substituted elements Co, aluminum (Al), copper (Cu), Ga, and Zr; and the basic elements iron (Fe) and boron (B). Machine oil is responsible for the carbon and hydrogen content in the centerless grinding sludge, which can be reduced in the RD process, as described in the next section. Although the centerless sludge has a high oxygen content, it is an ideal starting material for recycling into Nd–Fe–B sintered magnets through the RD process.

3.2. Calcium RD process

The calcium RD mechanism has been studied previously with commercial REEs oxide as the reactant [24–26]. However, to the best of our knowledge, use of the RD mechanism with Nd–Fe–B sludge as the starting material has not been reported. In this study, a range of reaction temperatures (600, 850, 950, and 1050 °C) was studied in order to determine the reaction kinetics during the RD process. Fig. 3 shows the XRD patterns, before and after washing, of the RD powders for different reaction temperatures, and Fig. 4 shows the SEM images of the RD powders, after washing, for different reaction temperatures. For the reaction temperature of 600 °C, a series of peaks can be identified as alpha-iron (α-Fe), neodymium oxygen chloride (NdOCl), and calcium chloride tetrahydrate ($CaCl_2{\cdot}4H_2O$) (Fig. 3(a), part (i)) before washing; however, no $Nd_2Fe_{14}B$ phase can be detected, which indicates that the tetragonal structure of $Nd_2Fe_{14}B$ was destroyed and the NdOCl phase was formed. After washing, the peaks of α-Fe and NdOCl appear distinctly in part (i) of Fig. 3(b). On the other hand, the Fe_3O_4 particles contained in the Nd–Fe–B sludge were reduced to Fe at 600 °C. The SEM image in Fig. 4(a) shows that numerous small particles have adhered to the larger particles, which differ from the sludge particles shown in Fig. 2(a). Since the temperature is lower than the melting point of calcium (839 °C), the calcium granules are not involved in the chemical reaction. In this stage, the $CaCl_2$ powder has already reacted with the sludge; this finding differs from what has previously been reported [27].

When a higher temperature was used (850 °C), some peaks of the $Nd_2Fe_{14}B$ phase were present (Fig. 3(a) part (ii) and (b) part (ii)), suggesting that the NdOCl phase was reduced and subsequently formed the $Nd_2Fe_{14}B$ phase because the reaction temperature reached the reactivity of calcium. At this stage, aggregation of small spherical particles on the surface of a large particle was clearly observed, as shown in Fig. 4(b). This is the beginning of the nucleation of the $Nd_2Fe_{14}B$ grains, which implies that the Nd and B atoms have diffused into the matrix of α-Fe particles to form $Nd_2Fe_{14}B$ grains. This finding aligns with the results reported by Chen et al. [28]. Despite the formation of the $Nd_2Fe_{14}B$ phase at 850 °C, distinct peaks from α-Fe can be seen in Fig. 3(b) part (ii),

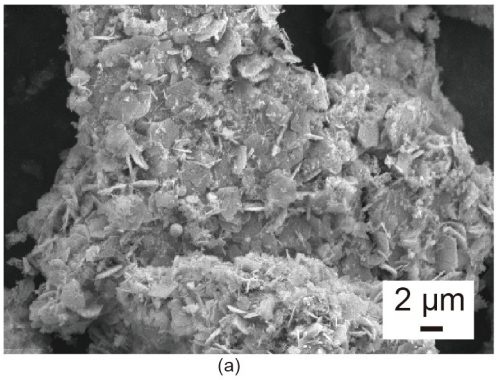

(a)

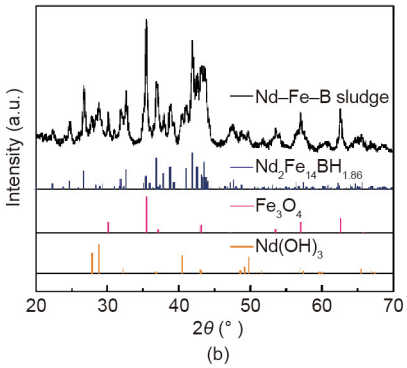

(b)

Element	Nd	Pr	Gd	Dy	Ho	Co	Al	Zr	Cu	Ga	B	Fe	H	O	RE
Starting sludge (wt%)	19.95	6.74	3.71	0.52	0.57	0.71	0.47	0.09	0.1	0.12	0.85	Bal	0.51	21.8	31.49

(c)

Fig. 2. Nd–Fe–B centerless grinding sludge dried at 60 °C for 2 h in air. (a) SEM secondary electronic image; (b) XRD pattern; (c) chemical composition of the sludge. RE: rare earth; Bal: balance.

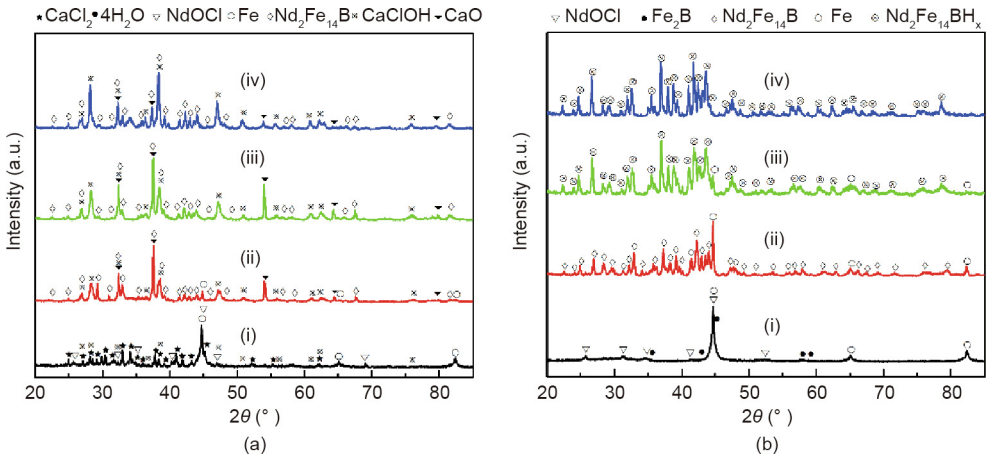

Fig. 3. XRD patterns of Nd–Fe–B sludge treated by the RD process with a calcium/sludge weight ratio of 50 wt% (a) before and (b) after removing CaO, for different reaction temperatures: (i) 600 °C; (ii) 850 °C; (iii) 950 °C; (iv) 1050 °C. Calcium granules were removed from the sample after annealing at 600 °C.

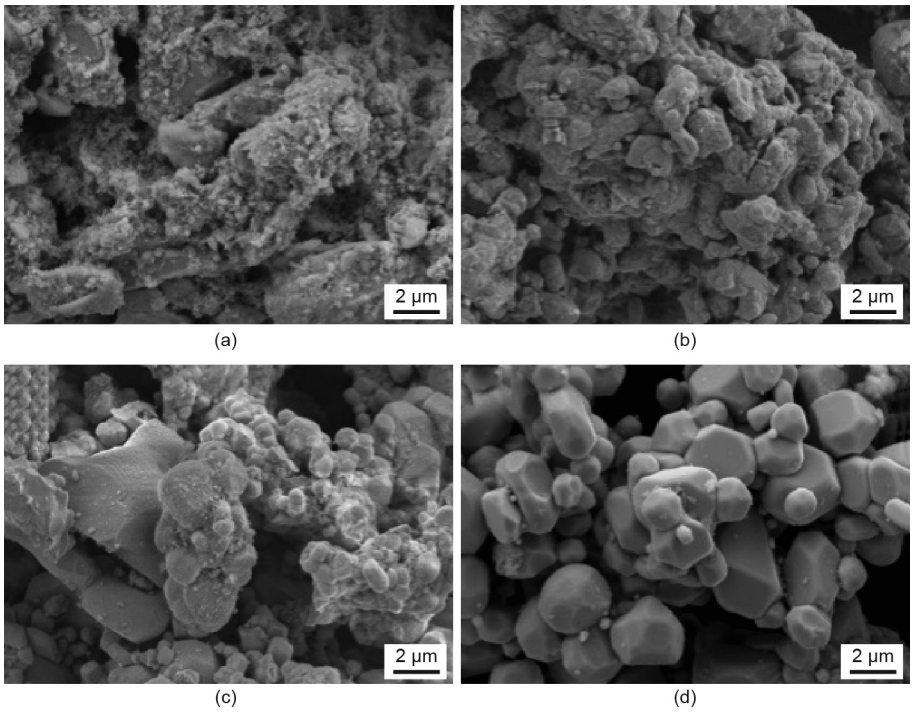

Fig. 4. SEM images of Nd–Fe–B sludge treated by the RD process with a calcium/sludge weight ratio of 50 wt% at different temperatures: (a) 600 °C; (b) 850 °C; (c) 950 °C; (d) 1050 °C.

implying that a higher reaction energy is needed to improve the nucleation driving force. It is also worth mentioning that peaks indicating CaClOH rather than $CaCl_2$ appear in Fig. 3(a) part (ii), which indicates that the $CaCl_2$ powder was involved in the chemical reactions. When the reaction temperature reached 950 °C, $Nd_2Fe_{14}B$ was obtained as the main phase, but a weak peak indicating the α-Fe phase remained in the XRD pattern, as shown in Fig. 3(b) part (iii). Nevertheless, more $Nd_2Fe_{14}B$ grains were present on the surface of a large particle, which did not have clear edges due to the low driving force of nucleation. Therefore, clean-cut and smooth-faced $Nd_2Fe_{14}B$ particles were clearly observed when the reaction temperature reached 1050 °C, as shown in Fig. 4(d).

Meanwhile, sharpened peaks can be seen in the XRD pattern of Fig. 3(b) part (iv), which indicate the single-phase of $Nd_2Fe_{14}B$. It is clear that reaction temperature is a crucial parameter when synthesizing $Nd_2Fe_{14}B$ particles from Nd–Fe–B sludge through the RD process. The sequence of each reaction during the RD process can be stated as follows:

Step 1:

$$Nd_2Fe_{14}BH_x + 4CaCl_2 + 2Nd(OH)_3 + 2H_2O = 4NdOCl + 4CaClOH + Fe_2B + 12Fe\left(\frac{x}{2}+3\right)H_2 \quad (1)$$

$$Fe_3O_4 + 4Ca = 3Fe + 4CaO \quad (2)$$

Step 2:

$$2NdOCl + 3Ca = 2Nd + CaCl_2 + 2CaO \quad (3)$$

$$CaO + H_2O = Ca(OH)_2 \quad (4)$$

$$Ca(OH)_2 + CaCl_2 = 2CaClOH \quad (5)$$

Step 3:

$$2Nd + 12Fe + Fe_2B = Nd_2Fe_{14}B \quad (6)$$

Step 4 (washing process):

$$Ca + 2H_2O = Ca(OH)_2 + H_2 \quad (7)$$

$$CaO + H_2O = Ca(OH)_2 \quad (8)$$

$$Nd_2Fe_{14}B + \frac{x}{2}H_2 = Nd_2Fe_{14}BH_x \quad (9)$$

To minimize the amount of calcium granules used in the RD process, a range of calcium/sludge weight ratios (20 wt%, 30 wt%, 40 wt%, and 50 wt%) were studied. Figs. 5 and 6 show the XRD patterns and SEM images of the washed samples after the RD process for different weight ratios of calcium/sludge. In the case of 20 wt%, the presence of the α-Fe phase can clearly be observed in Fig. 5(a), indicating that this amount of calcium is insufficient to reduce the total oxide contained in the starting materials. The irregular particles with good crystallinity shown in Fig. 6(a) were identified as α-Fe particles that had formed due to the high reaction temperature of 1050 °C. $Nd_2Fe_{14}B$ peaks appeared in the sample at 30 wt% of calcium; however, the presence of α-Fe peaks suggested that the sludge was not fully reduced by the calcium granules. In this sample, spherical particles of $Nd_2Fe_{14}B$ and irregular particles of α-Fe were concomitant, as shown in the SEM image (Fig. 6(b)). When the amount of calcium reached 40 wt%, only the $Nd_2Fe_{14}B$ phase was observed in the XRD pattern (Fig. 5(c)); furthermore, spherical particles of $Nd_2Fe_{14}B$ were observed (Fig. 6(c)), indicating that this amount of calcium was sufficient to remove the oxygen contained in the sludge. However, the $Nd_2Fe_{14}BH_x$ (x = 1–5) phase appeared instead of $Nd_2Fe_{14}B$ (Fig. 5(d)) when the calcium/sludge weight ratio reached 50 wt%, indicating that this amount of calcium was excessive. The residual calcium granules generated hydrogen (H_2) gas vigorously during the washing process with water (H_2O), and the hydrogen diffused interstitially into the lattice of $Nd_2Fe_{14}B$ to form $Nd_2Fe_{14}BH_x$ according to Eqs. (4) and (6). This finding is consistent with the results reported by Claude et al. [29]. Nevertheless, the obtained recycled particles maintained regular shapes, as shown in Fig. 6(d).

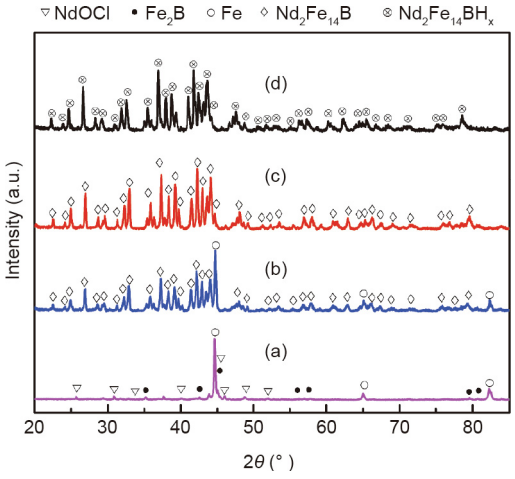

Fig. 5. XRD patterns of Nd–Fe–B powder treated by the RD process with different calcium/sludge weight ratios: (a) 20 wt%; (b) 30 wt%; (c) 40 wt%; (d) 50 wt%.

According to Fig. 2(c), the oxygen content in the sludge powder was 21.8 wt%, which—in theory—would consume the calcium granules at 54.5 wt%. However, this study showed that fewer calcium granules can fully reduce the sludge powder and form single-phase $Nd_2Fe_{14}B$, indicating that $CaCl_2$ plays an important role during the RD process. Due to the presence of oxygen and chlorine, oxychloride can easily be formed at high temperatures, and contributes to consuming oxygen. Furthermore, the melting point of $CaCl_2$ is lower than that of the calcium granules, so it provides a liquid system for the chemical reactions. Hence, the presence of $CaCl_2$ is beneficial for decreasing the overall calcium usage and improving the efficiency of the RD process in order to

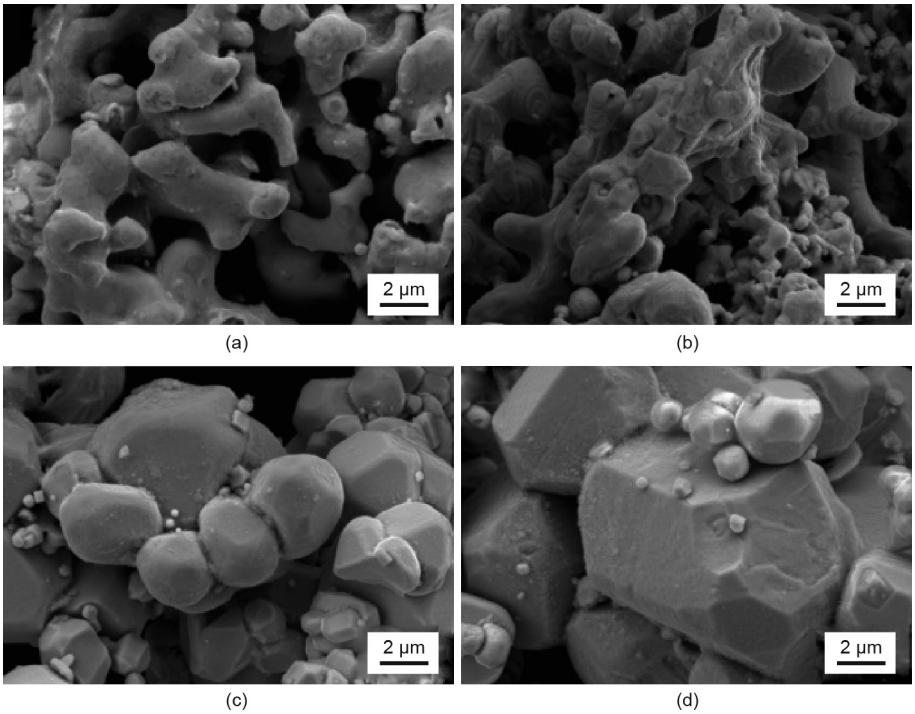

Fig. 6. SEM images of Nd–Fe–B powder treated by the RD process with different calcium/sludge weight ratios: (a) 20 wt%; (b) 30 wt%; (c) 40 wt%; (d) 50 wt%.

recoup the cost of recycling. In addition, the formation of $Nd_2Fe_{14}BH_x$ is more stable than that of $Nd_2Fe_{14}B$, which reduces corrosion [30]. As shown in Table 1, the carbon, hydrogen, and oxygen contents in the final product were 0.08 wt%, 0.22 wt%, and 0.42 wt%, respectively, indicating that the carbon content is reduced after the RD process. On the other hand, the most valuable elements contained in the sludge were efficiently recovered as recycled powders, as shown in Table 1, which is a merit of the calcium RD process with $CaCl_2$.

3.3. Preparation of recycled magnets and their magnetic properties

Recycled Nd–Fe–B powder was recovered from the Nd–Fe–B centerless grinding sludge through the RD process with 50 wt% calcium and 30 wt% $CaCl_2$ at 1050 °C for 2 h. Fig. 7(a) shows the SEM morphology of the RD powder. It can be observed that most of the particles are sphere-like crystals with diameters of less than 10 μm. However, the size distribution of the particles is rather wide. Further analysis through LPSA indicated that the particle size exhibits a bimodal distribution, with two mean diameters of 4 and 8 μm, as shown in the inset of Fig. 7(a). To prepare recycled magnets, ball milling was applied to the RD powder in order to achieve particles with uniform size distribution. After milling, most of the particles had equiaxed shapes, with an appropriate size distribution and a mean diameter of 3.5 μm, as shown in Fig. 7(b). In addition, the recycled powders had a rare earth content of 30.26 wt% and an oxygen content of 0.42 wt%, indicating that additional rare earth needed to be added in order to fabricate fully dense magnets. In previous studies, rare earth hydrides were blended with the powder when fabricating Nd–Fe–B sintered magnets [31,32]. However, the hydrides are easily oxidized in the ball-milling process, which reduces the utilization efficiency of the rare earth. In our previous studies, powders prepared from rare-earth-rich alloys proved to be effective additives for the fabrication of Nd–Fe–B sintered magnets with good magnetic properties [7,33]. Therefore, $Nd_4Fe_{14}B$ powder was prepared through the previously used method, yielding a good size distribution with a mean size of 3 μm, as shown in Fig. 7(c).

Recycled Nd–Fe–B sintered magnets were obtained by adding different amounts of $Nd_4Fe_{14}B$ powder, ranging from 33.3 wt% to 45.8 wt%. Fig. 8 shows the demagnetization curves of the recycled magnets. It can be observed that the curves exhibit good squareness, which is a necessary condition for their practical application. To compare the magnetic properties and density in detail, the obtained parameters are shown in the inset table of Fig. 8. It can be seen that the recycled magnets are fully dense and that their magnetic properties have reached the level of commercial sintered magnets. Moreover, it can be seen that the changes in the densities, remanences, and energy products are negligible when the additive amount of $Nd_4Fe_{14}B$ powder is increased linearly, as shown in Fig. 8. Furthermore, the coercivity increases slowly when the additive amount ranges from 33.3 wt% to 41.6 wt%, and subsequently decreases when the doping amount is 45.8 wt%.

For clarification, SEM images of recycled Nd–Fe–B magnets with additive ratios of 33.3 wt% and 45.8 wt%, respectively, are shown in Fig. 9. It can be observed that the microstructure of both magnets is similar, indicating that the magnets may possess similar magnetic properties. However, the rare earth and oxygen contained in the two magnets are quite different, as shown in Table 1. With an increasing rare earth content, the oxygen content of the recycled magnet increases, which undermines the coercivity and reduces the corrosion resistance of the magnet. In addition, redundant Nd-rich particles induce magnetic dilution and deteriorate the microstructure of the recycled magnets. On the other hand, reducing the amount of rare earth added during the recycling process can be part of a green design to cut the recycling cost and promote resource circulation. Nevertheless, minimizing the rare earth additive amount to obtain a recycled magnet with optimized magnetic properties during the recycling process is a goal for future research Fig. 9.

4. Conclusions

This paper presented an efficient recycling route for fabricating Nd–Fe–B sintered magnets from centerless grinding sludge, involving the calcium RD process and a rare-earth-rich alloy-doping

Table 1
Chemical composition of the recycled powder and magnets for different doping amounts of $Nd_4Fe_{14}B$ powder.

Specimen	Chemical composition (wt%)															
	Nd	Pr	Gd	Dy	Ho	Co	Al	Zr	Cu	Ga	B	Fe	C	H	O	RE
Recycled powders	19.30	6.30	3.60	0.55	0.51	0.76	0.5	0.050	0.11	0.12	0.85	Bal	0.08	0.22	0.42	30.26
Specimen A	27.15	4.70	2.35	0.65	0.34	0.50	0.5	0.050	0.08	0.08	0.80	Bal	0.05	0.09	0.58	35.19
Specimen B	27.75	4.50	2.15	0.65	0.33	0.48	0.5	0.050	0.07	0.08	0.75	Bal	0.06	0.08	0.62	35.38
Specimen C	28.85	4.30	2.00	0.65	0.30	0.44	0.5	0.050	0.07	0.08	0.75	Bal	0.04	0.07	0.78	36.10
Specimen D	30.20	4.25	1.90	0.65	0.29	0.43	0.5	0.035	0.07	0.08	0.75	Bal	0.05	0.07	0.86	37.29

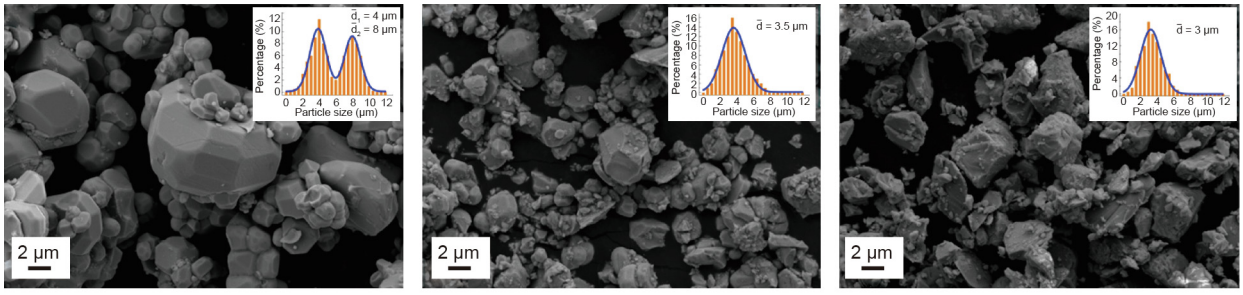

Fig. 7. SEM images of (a) RD powder, (b) recycled $Nd_2Fe_{14}B$ powder milled for 1.5 h, and (c) jet-milled $Nd_4Fe_{14}B$ powder. Inset is the particle size distribution of corresponding powders. $\bar{d}$ is the diameter of the particles.

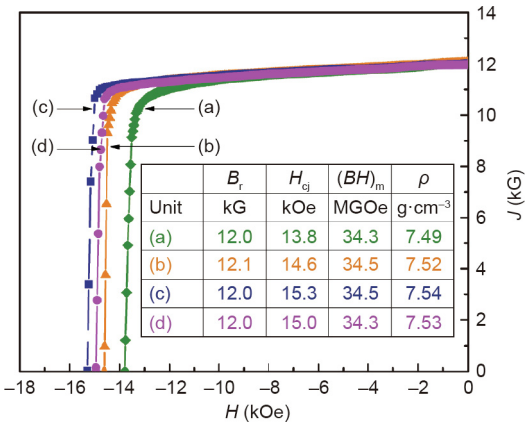

	B_r	H_{cj}	$(BH)_m$	ρ
Unit	kG	kOe	MGOe	g·cm^{-3}
(a)	12.0	13.8	34.3	7.49
(b)	12.1	14.6	34.5	7.52
(c)	12.0	15.3	34.5	7.54
(d)	12.0	15.0	34.3	7.53

Fig. 8. Demagnetization curves of recycled Nd–Fe–B magnets doped with $Nd_4Fe_{14}B$ powder: (a) 33.3 wt%; (b) 37.7 wt%; (c) 41.6 wt%; (d) 45.8 wt%. The inset table provides the corresponding properties of the magnets. *J*: magnetic polarization; *H*: magnetic field; B_r: remanence; H_{cj}: coercivity; $(BH)_{max}$: magnetic energy product; ρ: density.

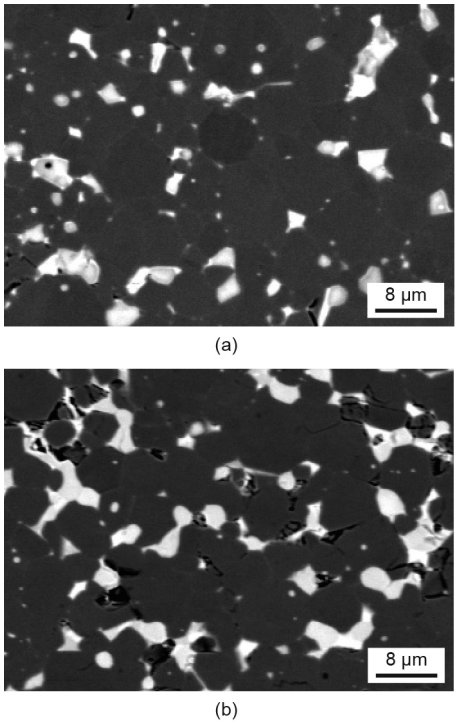

Fig. 9. SEM images of recycled magnets doped with different ratios of $Nd_4Fe_{14}B$ powder: (a) 33.3 wt%; (b) 45.8 wt%.

technique. To reduce the recycling cost and improve efficiency during the recycling process, the mechanism of the RD process and the role of the additive amount of $Nd_4Fe_{14}B$ powder were investigated. $CaCl_2$ powder played an important role as an assistant agent in promoting the efficiency of the chemical reaction. The Nd-rich alloy $Nd_4Fe_{14}B$ made a great contribution to the magnetic hardening of the recycled Nd–Fe–B sintered magnets, thereby making it possible to achieve good magnetic performance. The best magnetic properties, with a remanence of 12.1 kG, a coercivity of 14.6 kOe, and a maximum energy product of 34.5 MGOe, were obtained for a magnet doped with 37.7 wt% $Nd_4Fe_{14}B$ powder. The magnetic performance of the obtained magnets reached that of mid-level commercial Nd–Fe–B sintered magnets, indicating that the recycling technique described here provides a potential route for recycling Nd–Fe–B sludge into sintered magnets on a commercial scale.

Acknowledgements

This work was financially supported by the National High Technology Research and Development Program of China (2012AA063201), the Beijing Municipal Natural Science Foundation (2172012), and the State Key Laboratory of Rare Earth Permanent Magnetic Materials Opening Foundation (SKLREPM17OF02). Ming Yue is indebted to Professor Zaven Altounian of McGill University for very helpful discussions.

Compliance with ethics guidelines

Xiaowen Yin, Ming Yue, Qingmei Lu, Min Liu, Feng Wang, Yubing Qiu, Weiqiang Liu, Tieyong Zuo, Shanshun Zha, Xuliang Li, and Xiaofei Yi declare that they have no conflict of interest or financial conflicts to disclose.

References

[1] Gutfleisch O, Willard MA, Brück E, Chen CH, Sankar SG, Liu JP. Magnetic materials and devices for the 21st century: stronger, lighter, and more energy efficient. Adv Mater 2011;23(7):821–42.
[2] Jones N. Materials science: the pull of stronger magnets. Nature 2011;472(7341):22–3.
[3] Coey JMD. Hard magnetic materials: aperspective. IEEE Trans Magn 2011;47(12):4671–81.
[4] Nakamura H. The current and future status of rare earth permanent magnets. Scr Mater 2017;154:273–6.
[5] Dong SZ, Li W, Chen HS, Han R. The status of Chinese permanent magnet industry and R&D activities. AIP Adv 2017;7(5):056237.
[6] Itoh M, Miura K, Machida K. Novel rare earth recovery process on Nd–Fe–B magnet scrap by selective chlorination using NH_4Cl. J Alloys Compd 2009;477(1–2):484–7.
[7] Li XT, Yue M, Liu WQ, Li XL, Yi XF, Huang XL, et al. Large batch recycling of waste Nd–Fe–B magnets to manufacture sintered magnets with improved magnetic properties. J Alloys Compd 2015;649:656–60.
[8] Zakotnik M, Tudor CO. Commercial-scale recycling of NdFeB-type magnets with grain boundary modification yields products with "designer properties" that exceed those of starting materials. Waste Manag 2015;44:48–54.
[9] Takeda O, Okabe TH. Current status on resource and recycling technology for rare earths. Metall Mater Trans E 2014;1(2):160–73.
[10] Binnemans K, Jones PT, Blanpain B, Van Gerven T, Yang Y, Walton A, et al. Recycling of rare earths: a critical review. J Clean Prod 2013;51:1–22.
[11] Belova VV. Development of solvent extraction methods for recovering rare earth metals. Theor Found Chem Eng 2017;51(4):599–609.
[12] Jha MK, Kumari A, Panda R, Rajesh Kumar J, Yoo K, Lee JY. Review on hydrometallurgical recovery of rare earth metals. Hydrometallurgy 2016;161:77–101.
[13] Kim D, Powell LE, Delmau LH, Peterson ES, Herchenroeder J, Bhave RR. Selective extraction of rare earth elements from permanent magnet scraps with membrane solvent extraction. Environ Sci Technol 2015;49(16):9452–9.
[14] Vahidi E, Zhao F. Environmental life cycle assessment on the separation of rare earth oxides through solvent extraction. J Environ Manage 2017;203(Pt 1):255–63.
[15] Bian YY, Guo SQ, Jiang L, Tang K, Ding WZ. Extraction of rare earth elements from permanent magnet scraps by FeO-B_2O_3 flux treatment. J Sustain Metall 2015;1(2):151–60.
[16] Hua ZS, Wang J, Wang L, Zhao Z, Li XL, Xiao YP, et al. Selective extraction of rare earth elements from NdFeB scrap by molten chlorides. ACS Sustain Chem Eng 2014;2(11):2536–43.
[17] Sun GF, Chen JF, Dahl W, Klaar HJ, Burchard WG. The synthesis of Nd–Fe–Co–B by reduction–diffusion and its magnetic properties. J Appl Phys 1988;64(10):5519–21.
[18] Asabe K, Saguchi A, Takahashi W, Suzuki RO, Ono K. Recycling of rare earth magnet scraps: part I carbon removal by high temperature oxidation. Mater Trans 2001;42(12):2487–91.
[19] Suzuki RO, Saguchi A, Takahashi W, Yagura T, Ono K. Recycling of rare earth magnet scraps: part II oxygen removal by calcium. Mater Trans 2001;42(12):2492–8.
[20] Saguchi A, Asabe K, Takahashi W, Suzuki RO, Ono K. Recycling of rare earth magnet scraps part III carbon removal from Nd magnet grinding sludge under vacuum heating. Mater Trans 2002;43(2):256–60.
[21] Saguchi A, Asabe K, Fukuda T, Takahashi W, Suzuki RO. Recycling of rare earth magnet scraps: carbon and oxygen removal from Nd magnet scraps. J Alloys Compd 2006;408–412:1377–81.

[22] Yin XW, Liu M, Wan BC, Zhang Y, Liu WQ, Wu YF, et al. Recycled Nd–Fe–B sintered magnets prepared from sludges by calcium reduction–diffusion process. J Rare Earths 2018;36(12):1284–91.
[23] Yue M, Yin XW, Li XT, Li M, Li XL, Liu WQ, et al. Recycling of Nd–Fe–B sintered magnets sludge via the reduction–diffusion route to produce sintered magnets with strong energy density. ACS Sustain Chem Eng 2018;6(5):6547–53.
[24] Zhong Y, Chaudhary V, Tan X, Parmar H, Ramanujan RV. Mechanochemical synthesis of high coercivity $Nd_2(Fe,Co)_{14}B$ magnetic particles. Nanoscale 2017;9(47):18651–60.
[25] Lin JH, Liu SF, Cheng QM, Qian XL, Yang LQ, Su MZ. Preparation of Nd–Fe–B based magnetic materials by soft chemistry and reduction–diffusion process. J Alloys Compd 1997;249(1–2):237–41.
[26] Km CW, Km YH, Cha HG, Kang YS. Study on synthesis and magnetic properties of Nd–Fe–B alloy via reduction–diffusion process. Phys Scr 2007; T129:321–5.
[27] Chen CJ, Liu TY, Hung YC, Lin CH, Chen SH, Wu CD. Effect of $CaCl_2$ and $NdCl_3$ on the manufacturing of Nd–Fe–B by the reduction–diffusion process. J Appl Phys 1991;69(8):5501–3.
[28] Chen CQ, Kim D, Choi C. Influence of Ca amount on the synthesis of $Nd_2Fe_{14}B$ particles in reduction–diffusion process. J Magn Magn Mater 2014;355:180–3.
[29] Claude E, Ram S, Gimenez I, Chaudoüet P, Boursier D, Joubert JC. Evidence of a quantitative relationship between the degree of hydrogen intercalation and the coercivity of the two permanent magnet alloys $Nd_2Fe_{14}B$ and $Nd_2Fe_{11}Co_3B$. IEEE Trans Magn 1993;29(6):2767–9.
[30] Ram S, Joubert JC. Production of substantially stable Nd–Fe–B hydride (magnetic) powders using chemical dissociation of water. Appl Phys Lett 1992;61(5):613–5.
[31] Mottram RS, Kianvash A, Harris IR. The use of metal hydrides in powder blending for the production of NdFeB-type magnets. J Alloys Compd 1999;283 (1–2):282–8.
[32] Kianvash A, Mottram RS, Harris IR. Densification of a $Nd_{13}Fe_{78}NbCoB_7$-type sintered magnet by (Nd,Dy)-hydride additions using a powder blending technique. J Alloys Compd 1999;287(1–2):206–14.
[33] Li C, Liu WQ, Yue M, Liu YQ, Zhang DT, Zuo TY. Waste Nd–Fe–B sintered magnet recycling by doping with rare earth rich alloys. IEEE Trans Magn 2014;50(12):1–3.